

Modeling of hydration reactions using neural networks to predict the average properties of cement paste

Ki-Bong Park^{a,*}, Takafumi Noguchi^b, Joel Plawsky^a

^aDepartment of Chemical and Biological Engineering, Rensselaer Polytechnic Institute, Troy, NY 12180, USA

^bDepartment of Architecture, School of Engineering, The University of Tokyo, Tokyo, Japan

Received 12 February 2004; accepted 2 August 2004

Abstract

This paper presents a hydration model that describes the evolution of cement paste microstructure as a function of the changing composition of the hydration products. The hydration model extends an earlier version by considering the reduction in the hydration rate that occurs due to the reduction of free water and the reduction of the interfacial area of contact between the free water and the hydration products. The BP Neural Network method is used to determine the coefficients of the model. Using the proposed model, this paper predicts the following properties of hardening cement paste: the degree of hydration, the rate of heat evolution, the relative humidity and the total porosity. The agreement between simulation and experimental results proves that the new model is quite effective and potentially useful as a component within larger-scale models designed to predict the performance of concrete structures.

© 2004 Elsevier Ltd. All rights reserved.

Keywords: Modeling; Hydration; Kinetics; Microstructure; Physical properties

1. Introduction

1.1. General

Attempts have been made in the past to devise a kinetic model for cement reactions to predict the phenomena occurring in concrete, but the focus of these models has been on predicting the yield strength, the deformation under loading, and the cracking of sufficiently hardened concrete. The models have not yet reached the stage where they can explain the changes in the physical properties of concrete at very early ages. In recent years, the wide varieties of materials and requirements for structures have led to the extensive use of high strength and high performance concrete. This has emphasized the importance of knowing the early age physical properties during the process of hardening, such as the hydration heat, the autogenous

shrinkage, the creep and strength development, how these properties affect cracking at very early ages, and how these properties affect the durability after the concrete has hardened. Moreover, these early age phenomena affect one another and synergistically affect concrete. It is therefore difficult to explain the stress and cracking tendency of actual concrete structures with a model that describes a single physical property. To solve this problem, a universal model is necessary to comprehensively describe the early-age behavior of concrete. This work will present one such model that requires only a single correlating parameter. The simplicity of this model allows it to be incorporated into more sophisticated models, designed to predict the long-term performance of actual concrete structures.

1.2. Background and approach

In the past, several interesting concepts have been proposed to model the hydration processes and microstructural development in cement paste, mortar, and concrete. Many of these models are based on the “one single

* Corresponding author. Tel.: +1 518 276 2633; fax: +1 518 276 4030.
E-mail address: parkk@rpi.edu (K.-B. Park).

particle” construct that was proposed by Jander and Hoffman [1]. Jander et al. assumed that cement can be represented as “one single particle” and explained the reaction rate as a function of the degree of hydration (α) and time (t). The work of Kondo and Ueda [2], Tomosawa [3], Bezjack and Jelenic [4], Pommersheim and Clifton [5], Knudsen [6] and Osbaeck [7] also modeled the hydration rate using a single particle of cement. Jennings and Johnson [8] developed a microstructural model that considered the interaction between the hydrating particles. Pommersheim [9] considered the effects of particle size distribution (PSD) on the kinetics of hydration. Bents and Garboczi [10] proposed the three-dimensional digital-image-based simulation model of cement hydration that also showed the microstructure of the resulting concrete. Navi and Pignat [11] conducted a numerical simulation using an “Integrated Particle Kinetics Model”. van Breugel [12] explained the evolution of the hydration process and the microstructural development cement-based materials as a function of chemical composition and the particle size distribution of the cement. A consequence of these PSD approaches is that they require computation time to develop representative simulations and final properties. To be useful to design engineers, an approach based on a more statistical analysis is required. This will limit the computation time and allow for more time to be spent on the simulation of the actual concrete structure. Consequently, to predict the stress behavior and crack tendency in concrete members, a simple analytical approach is presented here.

In this paper, the hydration model proposed by Tomosawa [3,13] simulates the entire hydration process of cement paste using a single kinetic expression. The basic concepts of the model are based on a classic, shrinking, or unreacted core model [14]. However, this “unreacted core model” applies only to the case where a cement particle is immersed in an infinite pool of water. If the water to cement ratio is low, this model cannot properly explain the entire process of cement hydration. According to Powers’ [15] theory, for Portland cement to be completely hydrated, the water must be present in excess of 38% of the cement weight. If water is under the 38% limit, cement hydration will be incomplete due to the lack of free water and so a fraction of the cement will remain unreacted. To be successful, a hydration model must explain the decrease in the hydration rate when there is insufficient free water. Hyun [16] developed a hydration model that simulated the decrease in water concentration by expressing the reaction kinetics in terms of the degree of hydration and the water to cement ratio. Kishi and Maekawa [17] introduced a similar concept to simulate the reduction in the rate of heat evolution. In his model, the reduction in heat evolution was tied to the reduction of free water and the reduction of the layer thickness of internal hydrate. This in turn, led to a decrease in the contact area between the unreacted cement and the free water. The processes of heat evolution and hydration are interconnected since the rate of heat evolution is directly proportional to the reaction rate

and the reaction rate is an exponential function of the temperature. In this study, we model the reduction in the rate of heat evolution considering three mechanisms; the reduction of free water due to the increase in the extent of the hydration reaction, due to the decreased permeability of water through the hydration products, and due to the decrease in interfacial area between the unreacted cement and the free water. Estimating the resistance of the hydration product surrounding the anhydrous core to water penetration requires a model of the cement particle microstructure. In this paper, we present a microstructure model based on a unit cell that explains, via geometrical analysis, the growth of the hydration products. This model is coupled to a model of hydration kinetics that evaluates the reduction in heat evolution as a function of the free water content and the interfacial area between the free water and the unreacted cement.

The proposed hydration model includes four unknown coefficients, B , C , D , and k_r . Previously [18], the coefficients were obtained from fits to experimental data on the rate of heat evolution that we obtained using conduction calorimetry. In this paper, the coefficients are determined solely by feeding the material properties, mixture proportions, and environmental conditions into an artificial neural network. The hydration model used is a single function of the degree of hydration and includes the chemical and physical interactions between the hydration reactions, the microstructure, and the moisture content within the hardening cement paste. We solve the complete model numerically to predict the rate of heat evolution, the degree of hydration, and the total porosity of a hardening cement paste.

2. Modeling of hydration reaction

2.1. Hydration model

The hydration model [3,13] is expressed as a single equation composed of four rate coefficients. These coefficients determine the rate of formation and destruction of the initial impermeable layer, the activated chemical reaction process, and the following relevant, diffusion-controlled process. The model cement particle is assumed to be a sphere having an initial surface film composed of hydration products. External water diffuses through this layer, reacts with fresh cement, and then the newly formed hydration products diffuse outward. The process is considered to be mass transfer controlled so that the rate of water diffusion determines the hydration rate and is expressed as follows:

$$\frac{d\alpha}{dt} = \frac{3C_{w\infty}}{v\rho r_0^2} \frac{1}{\left(\frac{1}{k_d} - \frac{r_0}{D_e}\right) + \frac{r_0}{D_e}(1-\alpha)^{-1/3} + \frac{1}{k_r}(1-\alpha)^{-2/3}} \quad (1)$$

where α : degree of hydration; ν : stoichiometric ratio by mass of water to cement; ρ : density of unhydrated cement, r_0 : radius of unhydrated cement particle; D_c : effective diffusion coefficient of water in the cement gel; k_r : coefficient of reaction rate per unit area of reaction surface; $C_{w\infty}$: abundance concentration of water at the outer region of gel; k_d : mass transfer coefficient.

k_d is assumed to be a function of the degree of hydration to account for the change in permeability of the hydration products as the reaction progresses and is expressed as:

$$k_d = \frac{B}{\alpha^{1.5}} + C\alpha^3 \quad (2)$$

The effect of temperature on the hydration rate is introduced via the mass transfer coefficient. Accurate relationships are considered to be obtainable by experimentally determining the changes in the reaction rate. Here, it is assumed that B_{20} , C_{20} , D_{20} , and k_{r20} follow an Arrhenius-type law. The coefficients at T are expressed as follows:

$$\begin{aligned} B &= B_{20} \times \exp[-\beta_1(1/T - 1/293)] \\ C &= C_{20} \times \exp[-\beta_2(1/T - 1/293)] \\ D &= D_{20} \times \exp[-\beta_3(1/T - 1/293)] \\ k_r &= k_{r20} \times \exp[-E/R(1/T - 1/293)] \end{aligned} \quad (3)$$

where B_{20} , C_{20} , D_{20} , k_{r20} : frequency factors evaluated at 20 °C, T : absolute temperature (K); β_1 , β_2 , β_3 , E/R : reduced activation energies (K).

2.2. Microstructural model

To simplify this aspect of the overall model, the volume of the cement particle is assumed to be occupied by a mix of three components, unreacted cement, a composite hydration product, and capillary pores. The cement particles are assumed to be spherical, uniformly sized, and uniformly distributed throughout the cement paste. As hydration progresses, the hydration products grow uni-

formly at the surface of a cement particle and so the overall shape remains spherical over time. As shown in Fig. 1, the model is formulated geometrically in terms of a unit cell [19]. As the hydration products increase, the pore volume decreases. The basic elements of the model include the following.

The specific volume of unhydrated cement per 1 cm³ of cement paste, V_c , is:

$$V_c = \frac{1}{\chi\rho_c/\rho_w + 1} \quad (4)$$

where χ is water to cement ratio, ρ_c is the density of cement [g/cm³], and ρ_w is the density of water [g/cm³], and the average radius of a cement particle, r_0 :

$$r_0 = \frac{3}{S\rho_c} \quad (5)$$

where S is the specific surface area of cement [cm²/g]. From Eqs. (4) and (5), the number of cement particles in the paste, n is calculated as follows:

$$n = \frac{1}{(\rho_c\chi + 1)(4\pi r_0^3/3)} \quad (6)$$

Since the model is defined based on a cubic unit cell of paste, we transform the cement particle into an equivalent cube. The length of the cube that corresponds to the volume of cement paste is:

$$V = l^3 = \frac{1}{n} = (\rho_c\chi + 1)(4\pi r_0^3/3) \quad (7)$$

$$l = \sqrt[3]{4\pi(\rho_c\chi + 1)/3\rho_c} \quad (8)$$

The growth of hydration products can be expressed in the following way. When the cement particle is not in contact with an adjacent particle, the degree of hydration, α , is:

$$\alpha = 1 - \left[\frac{r_i}{r_0} \right]^3 \quad (9)$$

where r_i is the radius of the unhydrated cement particle ($=r_0-t$) and t is the layer depth of inner hydration

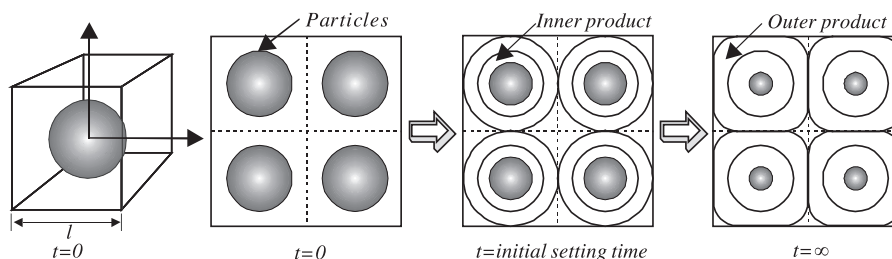


Fig. 1. Schematic of the growth of hydration product with hydration process.

products. The rate of volume growth of the hydration products, ξ , is:

$$\xi = \frac{R^3 - r_i^3}{r_0^3 - r_i^3} \quad (10)$$

where R is the radius of cement particle including the outer hydration products. From Eqs. (9) and (10), we find R as a function of the degree of hydration and the rate of volume growth:

$$R = [1 + (\xi - 1)\alpha]^{1/3} r_0 \quad (11)$$

In this paper, the rate of volume growth is assumed have a constant value of 2.0. Therefore, R can be calculated from the hydration model. As shown in Fig. 2, R changes gradually as the hydration reaction progresses. At any time, the pore volume, V_p , is assumed to be:

$$V_p = l^3 - V_s \quad (12)$$

where V_s is the volume of the cement particle including the outer hydration products. V_s changes gradually with R .

$$V_s = \frac{4}{3}\pi R^3, \quad R < \frac{l}{2} \quad (13)$$

$$V_s = \frac{4\pi R^3}{3} - 12\pi \left\{ \frac{2}{3}R^3 + \frac{l^3}{24} - \frac{R^2 l}{2} \right\}, \quad \frac{l}{2} < R < \frac{\sqrt{2}l}{2} \quad (14)$$

$$V_s = 2l^2 \sqrt{R^2 - \left(\frac{l}{2}\right)^2} + 16 \int_{\sqrt{R^2 - l^2/2}}^{l/2} S(x) dx, \quad \frac{\sqrt{2}l}{2} < R < \frac{\sqrt{3}l}{2} \quad (15)$$

where $S(x) = S_1 + S_2$

$$S_1 = \frac{l}{4} \sqrt{R^2 - \left(\frac{l}{2}\right)^2 - x^2},$$

$$S_2 = \frac{(R^2 - x^2)}{2} \left[\frac{\pi}{4} - \arccos\left(\frac{l}{2\sqrt{R^2 - x^2}}\right) \right]$$

The total porosity can be determined from:

$$\phi_p = \frac{V_p}{V_s} \quad (16)$$

where $V_s = l^3$.

2.3. Water reduction model

The water present in the paste can be classified into evaporable and non-evaporable fractions. The former is the capillary water and the gel water that resides partially within the hydration product. The non-evaporable water is defined as the bound water that is retained on D-dry [20]. However, the gel pore water cannot be easily distinguished from the capillary water due to the unsteady structure of the hydration products, particularly the C-S-H. To simplify the model, it is assumed that the evaporable water all resides in capillary pores and the non-evaporable water is bound water. The amount of bound water can be obtained by an ignition loss experiment but it also can be calculated from the degree of hydration, α , and the maximum bound water that exists in fully hydrated cement, W_n .

$$W_n(t) = W_n \alpha(t) \quad (17)$$

Here, $W_n(t)$ is the amount of bound water in 1 g of cement at time t and W_n is defined based on the composition of the cement clinker.

$$W_n = w_1(C_3S) + w_2(C_2S) + w_3(C_3A) + w_4(C_4AF) \quad (18)$$

C_3S , C_2S , C_3A and C_4AF represent the clinker mineral composition of cement and w_1 , w_2 , w_3 , w_4 are the amounts of bound water per gram of the individual constituents. The w 's are assumed to be w_1 : 0.234, w_2 : 0.178, w_3 : 0.514, w_4 : 0.158 [21].

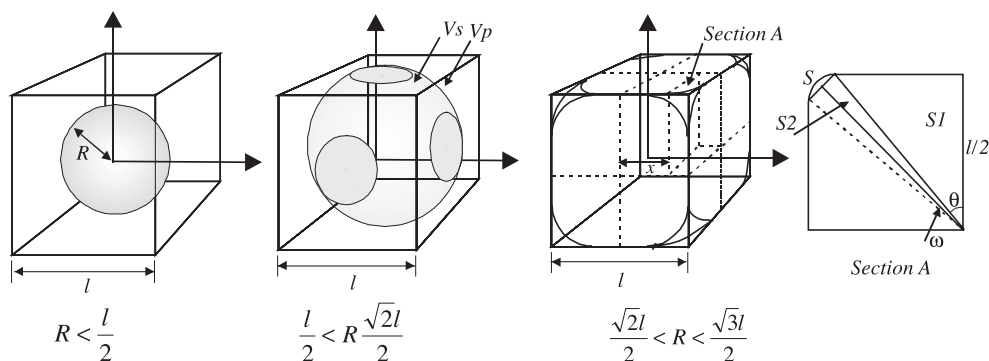


Fig. 2. Microstructure formation as a function of the growth of hydration products.

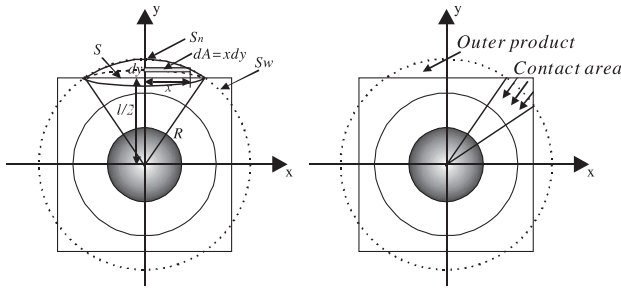


Fig. 3. Schematic diagram of the contact areas between free water and hydration products.

The free water is assumed to reside only in the capillary pores and is calculated by difference from the initial amount of water and the bound water. The amount of free water per 1 cm³ of cement paste, W_f , is then:

$$W_f = W_i - W_n(t)C_i \quad (19)$$

Here, W_i is the initial amount of water per 1 cm³ of the paste and C_i is the amount of cement per 1 cm³ of the paste. The relation between the free water and the relative humidity is determined by applying the absorption potential theory proposed by Halsey [22]. The relative humidity, RH, is thus:

$$W_f = a(\ln RH)^{-b} \quad (20)$$

$$RH = \exp \left[\left(\frac{a}{W_f} \right)^{1/b} \right] \quad (21)$$

where a and b are coefficients whose values are 22.0 and 0.05, respectively. Parrott et al. [23] proposed a relationship between the relative humidity, RH, and the reduction coefficient of reaction water, β_{RH} .

$$\beta_{RH} = \left[\frac{RH - 0.55}{0.45} \right]^4, \quad RH > 0.55 \quad (22)$$

$$\beta_{RH} = 0, \quad RH \leq 0.55 \quad (23)$$

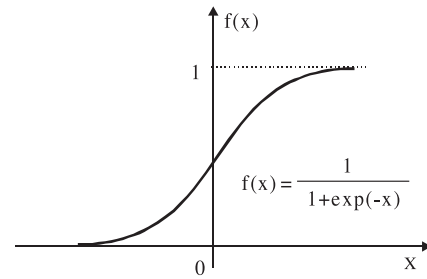


Fig. 5. Sigmoid function.

β_{RH} can be applied to the hydration model as follows:

$$C_{w1} = \beta_{RH} C_{w\infty} \quad (24)$$

where C_{w1} is an imaginary concentration of water that contributes to hydration.

2.4. Interfacial area between free water and hydration products

Permeability changes in the hydration products as the hydration reaction proceeds can be explained using the consumption of free water during the hydration process and the corresponding change in the microstructure of the particle. Fig. 3 shows a schematic diagram of how the volumes of the hydration products and the cement particle change within the unit cell of the paste. At the start of the hydration process, the surface of the cement particle has enough water for hydration to proceed but the free water has difficulty reaching cement in the interior due to the presence of the hydration product. As the hydration proceeds, the cement particle grows gradually as shown in Fig. 2. When the hydration products surrounding individual cement particles are not in contact with each other, the interfacial area between the free water and the cement particle is:

$$S_w = 4\pi R^2, \quad R < \frac{l}{2} \quad (25)$$

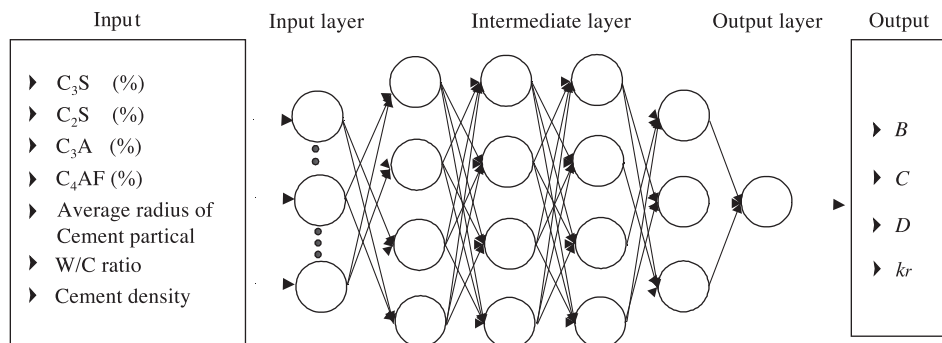


Fig. 4. Perception neural networks.

Table 1
Input layer of neural networks

Spec. no.	W/C	Specific gravity (g/cm ³)	Mineral composition (%)				Radius (μm)
			C ₃ S	C ₂ S	C ₃ A	C ₄ AF	
OPC	0.23, 0.28, 0.33, 0.5	3.16	62	15	8	9	6.18
HL1	0.5	3.20	37	43	4	9	7.86
HL3	0.5	3.20	34	48	4	7	7.19
L8	0.5	3.22	22	58	3	10	8.98
L10	0.5	3.22	17	70	2	6	8.02

If the hydration products around the particles are in contact with each other:

$$S_w = 4\pi R^2 - 12\pi \left\{ \left[R^2 \frac{\pi}{2} \right] - \left[\frac{l}{2} \sqrt{R^2 - \left(\frac{l}{2} \right)^2} + R^2 \sin^{-1} \frac{l/2}{R} \right] \right\}, \quad \frac{l}{2} < R < \frac{\sqrt{2}l}{2} \quad (26)$$

As the cement particle grows further, the interfacial area becomes:

$$S_w = 8 \int_0^{1/2} 2\sqrt{R^2 - x^2} \left[\frac{\pi}{4} - \arccos \left(\frac{l}{2\sqrt{R^2 - x^2}} \right) \right], \quad \frac{\sqrt{2}l}{2} < R < \frac{\sqrt{3}l}{2} \quad (27)$$

It is assumed that the hydration rate decreases as the interfacial area is reduced. The reduction of interfacial area is expressed in terms of the concentration of water in the bulk via the hydration model.

$$C_{w2} = \eta C_{w\infty} \quad (28)$$

where η : efficiency of reduction in contact area; $C_{w\infty}$: concentration of water in the bulk; C_{w2} : imaginary concentration of water that participates in the hydration reaction.

The relationship between η and R is given by:

$$R < \frac{l}{2}, \quad \eta = 1 \quad (29)$$

$$\frac{l}{2} < R < \frac{\sqrt{3}l}{2}, \quad \eta = 1 - \frac{S_w}{4\pi \left(\frac{l}{2} \right)^2} \quad (30)$$

Table 2
Calculated coefficients for the hydration model using neural networks

Spec	W/C	B ₂₀	C ₂₀	D ₂₀	k _{r20}	β ₁	β ₂	β ₃	E/R
OPC	0.5	3.50e-10	2.82e-2	3.00e-11	2.50e-6	9	804	5942	6000
OPC	0.33	3.50e-10	2.26e-2	3.00e-11	2.50e-6	9	804	5942	6000
OPC	0.28	3.50e-10	1.98e-2	3.00e-11	2.50e-6	9	804	5942	6000
OPC	0.23	3.50e-10	1.71e-2	3.00e-11	2.50e-6	9	804	5942	6000
HL1	0.5	3.65e-10	1.82e-3	4.00e-11	2.50e-6	12	800	3600	4230
HL3	0.5	3.80e-10	2.00e-4	5.50e-11	9.50e-6	89	545	3510	5220
L8	0.5	3.86e-10	1.25e-4	6.30e-11	8.50e-6	105	210	5200	2250
L10	0.5	3.92e-10	0.71e-4	6.80e-11	6.80e-6	8	450	5900	4842

2.5. Determination of hydration model coefficients using a neural network model

The coefficients for the formulation of the hydration model are determined by inputting the pertinent data on the materials, the mixture proportions and the environmental conditions into an artificial neural network. In this study, a multi-input–single-output, Back Propagation Network was used [24]. This network has four intermediate layers shown in Fig. 4. A sigmoid function (Fig. 5) that spans a range between [0,1] was used as the input–output function of the individual neural units [25]. The sigmoid function is expressed as follows:

$$f(x) = 1 / \{1 + \exp(-\psi x - \theta)\} \quad (31)$$

In Eq. (31), ψ is 1.0 and θ is 0.0. The number of units in the input layer is 7, and the number of units in the intermediate layers is 15 (4, 4, 4, and 3). An error back propagation method was adopted as the learning algorithm. The sign of the training data for the neural network is 35. Table 1 shows the data fed to the input layer of the network. The input data values include the mineral composition of the cement (C₃S, C₂S, C₃A, C₄AF), the average radius of the cement particles, the cement density and the water to cement ratio. The kinetic factors B , C , D , and k_r of the hydration model are given by the output of the net. The effect of temperature on the hydration rate is then introduced using Eq. (3), to determine the reduced activation energies, β_1 , β_2 , β_3 , and E/R . The coefficients of the hydration model determined from the output of the neural net are given in Table 2.

3. Results and discussion

3.1. Degree of hydration

Two types of cement were used in this study, ordinary Portland cement (OPC) and a belite-rich Portland cement (BPC). Cement paste was proportioned to have a water–cement ratio of 0.25 and 0.30 [26]. The percentage of bound water contained in the hydrates resulting from the reaction of cement with water was assumed to be the

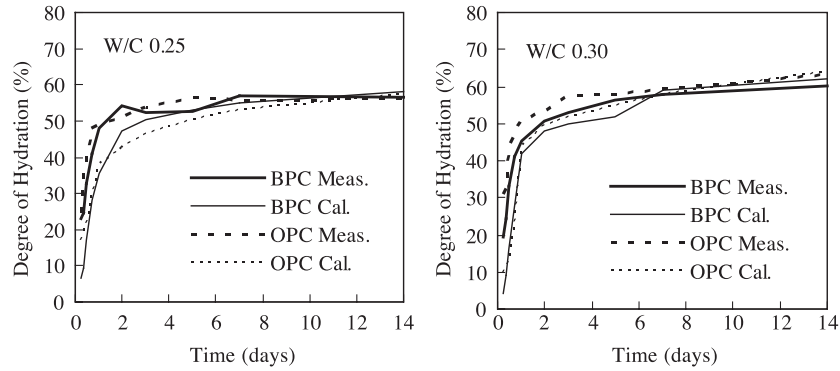


Fig. 6. Comparison of calculated and measured the degree of hydration.

degree of hydration. The degree of hydration was determined by assuming that the quantity of bound water was the same as the ignition loss at 1050 °C. The quantity of bound water at 100% hydration of the cement paste was determined by obtaining the amount of clinker-hydrate according to Bogue’s [1] method. Thus, when 1 g of cement fully reacts with water, the determined quantities of bound water for ordinary Portland cement and belite-rich cement were 0.254 and 0.276, respectively. Fig. 6 shows the changes in the degree of hydration with age. The model predicts a slightly smaller degree of hydration than the experiments at early ages.

3.2. Heat evolution rate

To verify the heat evolution aspects of the proposed model, experiments were performed using conduction calorimetry at 20 °C. Fig. 7 shows the effect of water to cement ratio on the rate of heat evolution using ordinary Portland cement. The model simulations and experimental results are in good agreement for all water to cement ratios. Fig. 8 shows the rate of heat evolution of a belite-rich cement having a different mineral composition from the cement used in Fig. 7. Good agreement between experiment and the model simulation is evident here as well.

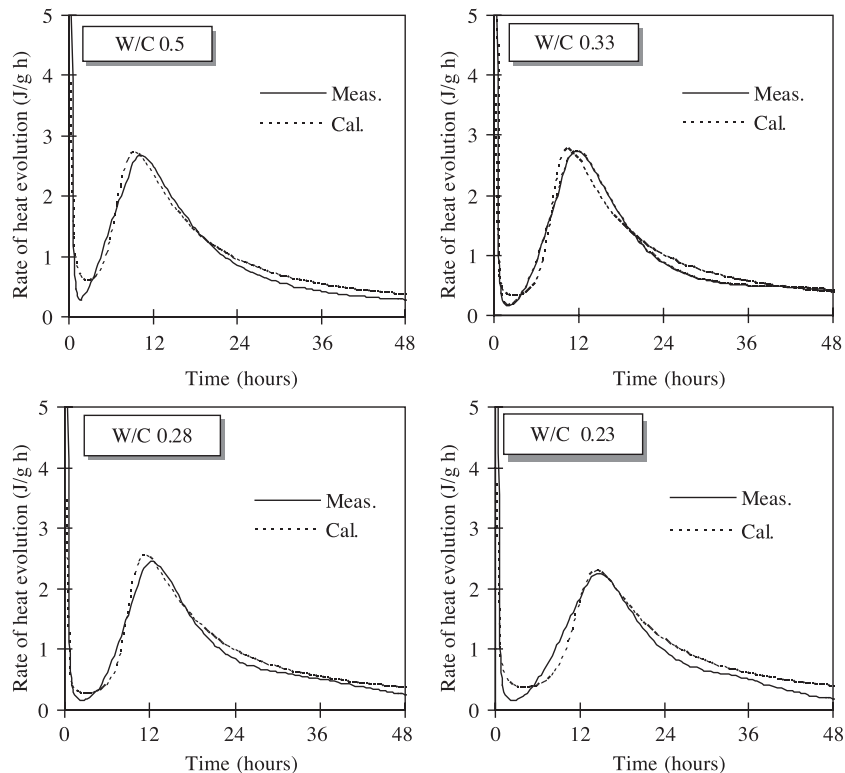


Fig. 7. Comparison of calculated and measured the rate of heat evolution for OPC.

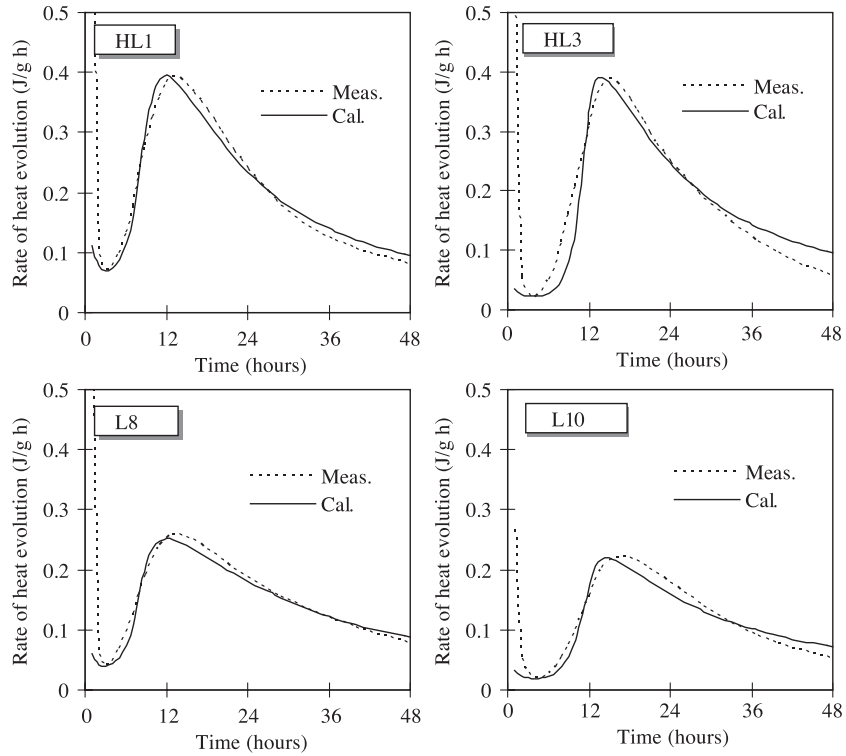


Fig. 8. Comparison of calculated and measured rate of heat evolution for BPC.

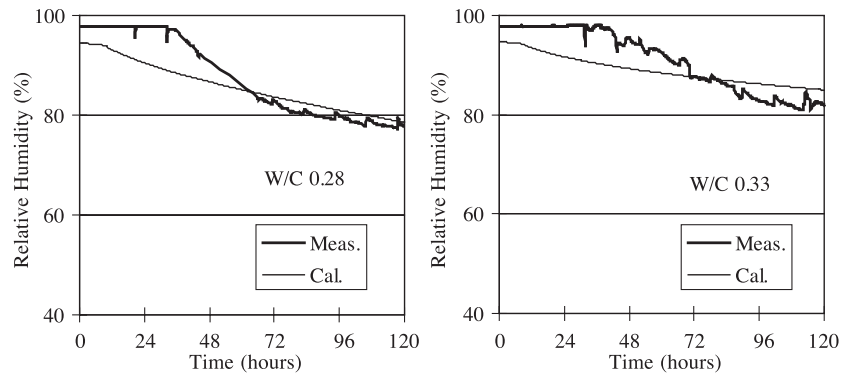


Fig. 9. Comparison of calculated and measured the relative humidity for OPC.

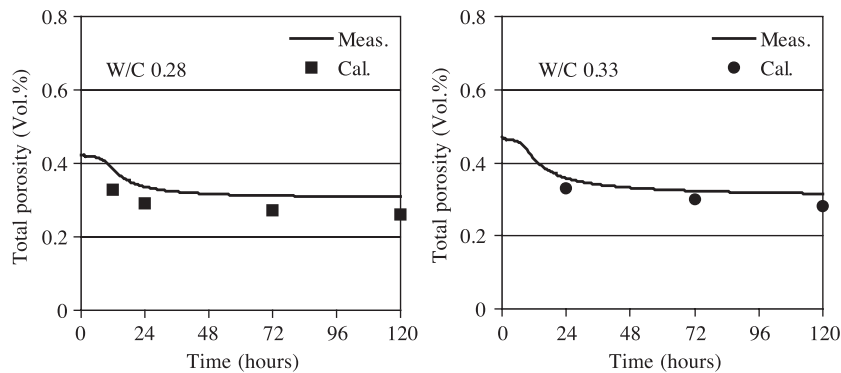


Fig. 10. Comparison of calculated and measured the total porosity for OPC.

3.3. Relative humidity and total porosity

To assess the relative humidity in the experimental samples, the relative humidity was measured in the center of a sealed $40 \times 40 \times 160$ -mm specimen [27]. The porosity of the samples was determined using mercury intrusion porosimetry. Fig. 9 shows the comparison between model simulations and measured values for the relative humidity. The model underestimates the relative humidity at early ages for both mixtures and this prediction is mirrored by a similar underestimation of the degree of hydration. Fig. 10 shows the model simulation and experimental results for the porosity of the paste. Here, the model overestimates the porosity at early ages. Though the model does not reproduce the experimental results exactly, both are in reasonable agreement.

4. Conclusions

A mathematical model, based on a single kinetic equation to predict the extent of hydration and the microstructure evolution of a cement particle, was developed. To test the validity of the model, predictions from the model for an ordinary Portland cement and a belite-enriched Portland cement were compared with experimental data. The results from the model were in good agreement with the experimental data and so the model developed here can be applied to the prediction of the mechanical properties of cement paste. The simplicity of the model will allow it to be incorporated into much larger simulations designed to predict the performance of actual concrete structures.

References

- [1] R.H. Bogue, *The Chemistry of Portland Cement*, 2nd ed., Reinhold Publishing, New York, 1955.
- [2] R. Kondo, S. Ueda, Kinetics and mechanisms of the hydration of cements, in: Proc. 5th Int. Cong. Chemistry of Cement, The Cement Association of Japan, Tokyo, vol. II, 1968, pp. 203–255.
- [3] F. Tomosawa, Kinetic hydration model of cement, in: Proc. Cem. and Concr., vol. 28, The Cement Association of Japan, 1974, pp. 53–57.
- [4] A. Bezjak, I. Jelenic, On the determination of rate constants for hydration process in cement pastes, *Cem. Concr. Res.* 10 (4) (1980) 553–563.
- [5] J.M. Pommersheim, J.R. Clifton, Mathematical modeling of tricalcium silicate hydration: II. Hydration sub-models and the effect of model parameters, *Cem. Concr. Res.* 12 (1982) 765–772.
- [6] T. Knudsen, The dispersion model for hydration of Portland cement: I. General concepts, *Cem. Concr. Res.* 14 (5) (1984) 622–630.
- [7] B. Osbaeck, Prediction of cement properties from description of the hydration processes, 9th Int. Cong. Chemistry of Cement, National Council for Cement and Building Materials, New Delhi, 1992, pp. 504–510.
- [8] H.M. Jennings, S.K. Johnson, Simulation of development during the hydration of a cement compound, *J. Am. Ceram. Soc.* 69 (11) (1986) 790–795.
- [9] J.M. Pommersheim, Effect of particle size distribution on hydration kinetics, in: L.J. Struble, P.W. Brown (Eds.), *Mat. Res. Symp. Proc.*, vol. 85, 1987, pp. 301–306.
- [10] D.P. Bentz, E.J. Gaboczi, Percolation of phases in a three-dimensional cement paste microstructural model, *Cem. Concr. Res.* 21 (1991) 325–344.
- [11] P. Navi, C. Pignat, Simulation of cement hydration and the connectivity of the capillary pore space, *Adv. Cem. Based Mater.* 4 (1996) 58–67.
- [12] K. van Breugel, Numerical simulation of hydration and microstructural development in hardening cement-based materials (I) theory, *Cem. Concr. Res.* 25 (2) (1995) 319–331.
- [13] F. Tomosawa, Development of a kinetic model for hydration of cement, in: F.S. Glasser, H. Justnes (Eds.), *Proc. 10th Int. Cong. Chemistry of Cement*, Gothenburg, vol. II, 1997, 2ii051 8 pp.
- [14] K.J. Hashimoto, *Reaction Engineering*, 2nd ed., Baifukan, Tokyo, 1993.
- [15] T.C. Powers, Properties of cement paste and concrete, paper V–I: physical properties of cement paste, in: Proc. 4th Int. Sym. on the Chemistry of Cement, Washington DC, vol. 2, 1960, pp. 577–613.
- [16] C. Hyun, Prediction of thermal stress of high strength concrete and massive concrete, PhD thesis, The University of Tokyo, Japan, 1995.
- [17] T. Kishi, K. Maekawa, Multi-component model for hydration heat of blend cement based on cement mineral compounds, in: T. Uomoto (Ed.), *Proc. JCI Sym. on Chemical Reaction and Process Analysis of Cement Concrete*, Tokyo, 1996, pp. 21–28.
- [18] C. Hyun, T. Noguchi, F. Tomosawa, Prediction of temperature rise and cracking in concrete members based on kinetic hydration model of cement, *Proc. Cem. Concr. Japan Cement Association* 619 (1998) 34–40.
- [19] K.-B. Park, Prediction of cracking in high strength concrete using a hydration model, PhD thesis, The University of Tokyo, Japan, 2001.
- [20] H.F.W. Taylor, *Cement Chemistry*, 2nd ed., Thomas Telford, London, 1997.
- [21] K. van Breugel, Simulation of hydration and formation of structure in hardening cement-based materials, PhD thesis, TU Delft, The Netherlands, 1991.
- [22] A. Baba, The mechanism of dry shrinkage of cement based materials, PhD thesis, The University of Tokyo, Japan, 1975.
- [23] L.J. Parrott, D. Killoh, R. Patel, Cement hydration under partially saturated condition, in: Abla Grafica (Ed.), *Proc. 8th Int. Cong. Chemistry of Cement*, Rio de Janeiro, vol. III, 1986, pp. 46–50.
- [24] S.E. Fahlman, Faster learning variation of back propagation: an empirical study, in: D. Touretzky, G.E. Hinton, T.J. Sejnowski (Eds.), *Proc. The 1988 Connectionist Models Summer School*, Morgan Kaufmann Publishers, California, 1988, pp. 38–51.
- [25] E.B. Baum, H. David, What size net gives valid generalization? *Neural Comput.* 1 (1) (1989) 151–160.
- [26] K.-B. Park, T. Noguchi, F. Tomosawa, A study of the hydration rate and autogenous shrinkage of cement paste, in: E. Tasawa (Ed.), *Proc. Autoshink'98, Int. Workshop on Autogenous Shrinkage of Concrete*, E&FN Spon, London, 1999, pp. 281–290.
- [27] K.-B. Park, T. Noguchi, Autogenous shrinkage of cement paste hydrated at different temperatures: influence of microstructure and relative humidity change, in: B. Persson, G. Fagerlund (Eds.), *Proc. 3rd Int. Seminar, Self-desiccation and its importance in concrete technology*, Lund University, Sweden, 2002, pp. 93–101.